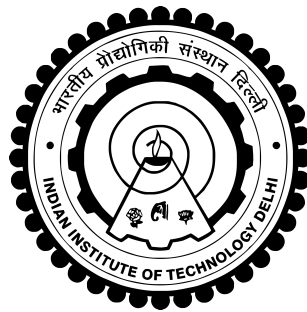


# **OPTIMAL BEAMFORMING STRATEGIES AT MMWAVES FOR 5G+ NETWORKS**

**NANCY VARSHNEY**



**BHARTI SCHOOL OF TELECOMMUNICATION  
INDIAN INSTITUTE OF TECHNOLOGY DELHI**

**APRIL 2023**

© Indian Institute of Technology Delhi (IITD), New Delhi, 2023

# **OPTIMAL BEAMFORMING STRATEGIES AT MMWAVES FOR 5G+ NETWORKS**

*by*

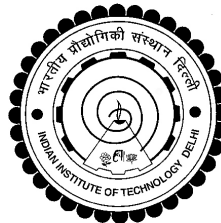
**NANCY VARSHNEY**

**Bharti School of Telecommunication**

Submitted

in fulfillment of the requirements of the degree of Doctor of Philosophy

to the



**INDIAN INSTITUTE OF TECHNOLOGY DELHI**

**APRIL 2023**

## Certificate

This is to certify that the dissertation entitled **Optimal Beamforming Strategies at mmWaves for 5G+ Networks**, submitted by **Ms. Nancy Varshney**, a Research Scholar, in the *Bharti School Of Telecommunication, Indian Institute of Technology Delhi, New Delhi, India*, for the award of the degree of **Doctor of Philosophy**, is a record of an original research work carried out by her under my supervision and guidance. The dissertation fulfills all requirements as per the regulations of this Institute and in my opinion has reached the standard needed for submission. Neither this dissertation nor any part of it has been submitted for any degree or academic award elsewhere.

**Prof. Swades De**

(Supervisor)

Department of Electrical Engineering

Indian Institute of Technology Delhi

New Delhi, 110016, India.

# Acknowledgements

First and foremost, thanks to the Almighty for showering his blessings on me that have helped in accomplishing this dissertation.

I would then like to express my sincere gratitude to my supervisor, Prof. Swades De, for giving me an opportunity to pursue Ph.D. at IIT Delhi. His passion for academia, discipline, and determination towards his work has always motivated me to work harder. His continuous guidance, valuable advice, and confidence in our pursued research work led to the fruition of this dissertation. It was a great privilege and honor to work under his supervision. I am extremely thankful to him for presenting me the opportunity to work as visiting scholar at Aalto University, Finland.

I would like to present my sincere gratitude to Prof. Riku Jäntti for his insightful advice during my research at Aalto University, Finland. I would then like to thank my committee members, Prof. Sheshan Srirangajan, Prof. Prof. Aparna Mehra, and Prof. Arpan Chattopadhyay for their valuable suggestions that have helped address important aspects in this dissertation.

I take this opportunity to thank Prof. K.V.S Srinivas from IIT (BHU) Varanasi for encouraging me to pursue career in research. I would like to thank my colleagues Dr. Suraj Suman, Dr. Vini Gupta, Mr. Ashutosh Balakrishnan, Ms. Ragini Jain, Ms. Kirandeep, and Dr. Farheen Chisti at IIT Delhi for their friendly support during this journey. I would also like to thank Dr. Reza Ghazalian at Aalto University, for having intellectual discussion that strengthened my research aptitude. I am grateful to all my seniors, lab-mates of the Communication Networks Research Group (CNRG), and friends at IIT Delhi, whose cooperation and encouragement have made this journey a memorable one.

Most importantly, I profoundly thank my parents, Mr. Avdhesh Varshney and Mrs. Sarita Varshney, my brother Mr. Shubham Varshney, my sister-in-law Mrs. Nidhi Varshney and the other family members for their consistent support, and encouragement during my Ph.D. study. Without their constant support and inspiration, this acknowledgment and PhD dissertation would have never appeared. I am indebted to the sacrifices my parents

have made to shape my career and I dedicate this dissertation to them.

**Nancy Varshney**  
(2018BSZ8118)

# Abstract

Beyond fifth generation (5G+) communication aims to provide a 3-dimensional ubiquitous network to support high data rates caused by device proliferation. To aid 5G+ communications, three spectrum bands are being investigated: sub-6 GHz, millimeter-wave (mmWave), and terahertz frequencies. Higher frequency range has the advantage of increased bandwidth availability, but it also has its own set of challenges such as increased signal attenuation, reduced cell range, increased computational and hardware complexities, and increased hardware cost. However, substantial research has been conducted to demonstrate the feasibility of communication at higher frequencies. This dissertation focuses specifically on mmWave-enabled communications for serving users under different 2-dimensional as well as 3-dimensional network. The number of radio frequency (RF) chains that can be deployed at a device is a bottleneck in the mmWave range due to high hardware power consumption and hardware complexity. This, in turn, presents challenges in designing precoders and combiners, parameter estimation, signal processing, and user scheduling. Therefore, the objective of this dissertation is to investigate and design energy and spectrally efficient reduced complexity terrestrial and aerial mmWave communications frameworks/architectures with a limited number of RF chains.

The first topic investigates sectorized-cell framework for a 2-dimensional multi-user terrestrial mmWave communications when the user population exceeds the number of RF chains available at the gNodeB. This framework is analyzed in the context of a single RF chain that serves all sectors of a cell in a round-robin manner with equal sector sojourn time. The idea is to partition the cell into identical sectors and serve multiple users simultaneously that fall within each sector at a given epoch using a single steerable beam generated from a uniform linear antenna array coupled to an RF chain at the gNodeB. Consequently, a large number of users are served with a limited number of RF chains. An optimization problem is formulated for combined resource allocation of orthogonal frequency division multiple (OFDM) symbols to users in a sector and sector beamwidth optimization in order to maximize average long-term user rate and system energy efficiency. Through simulation results, it is verified that serving multiple users over orthogonal frequency division multiple access with a single RF chain a sectorized cell system model achieves better performance than serving single user per RF chain at a time. Additionally, the effect of localization error on the optimum beamwidth, which results from position estimation, is also studied.

The second part of the dissertation extends the study of the sectored-cell framework with a single RF chain to the case of multiple RF chains at gNodeB. Because of its low complexity, the sub-array based or partially connected hybrid precoder is considered, in which each RF chain, connected to a separate antenna array, generates one steerable beam. Notably, the presence of sidelobes causes inter-beam interference when concurrent beams are generated from multiple RF chains. Therefore, the optimal beamwidth is estimated while accounting for inter-beam interference and beam squint. Furthermore, an optimal number of RF chains at the gNodeB is estimated by accounting for power waste in RF units. A variable time frame structure for the sectored-cell framework is also proposed for a standalone mmWave communications system with variable transmission time interval units as short as one OFDM symbol long. The frame structure for enhanced mobile broadband (eMBB) services is typically made up of slots with a fixed number of OFDM symbols, and the smallest transmission time interval unit is equivalent to one slot duration, as defined by the 3rd Generation Partnership Project (3GPP) New Radio (NR) in Release 15. Furthermore, 3GPP guidelines have suggested a separate beam management phase for the initial gNodeB-user beam pair to establish the best gNodeB-user beam pair to be used for subsequent data transfer in data transmission mode. During the beam management phase, narrow beams must scan the area multiple times before granting users channel access. As a result, using a fixed frame structure along with separate beam management and data transmission phase causes significant initial access delays. Furthermore, because beam training overhead is often low for beam search operations, the wideband mmWave channel is underutilized during the beam training phase. Therefore, a modified sector-wise initial access procedure is proposed, which offers decreased initial access delay and increased bandwidth utilization. The proposed variable time frame structure, along with the modified initial access procedure, offers an improved average and the geometric mean of long-run user rates, especially in the case of non-homogeneous user distribution in the area.

The third part of the dissertation studies in detail the effect of beam squint in wideband mmWave communication. The beam squint effect is caused by the use of a large number of antenna elements connected per RF chain to generate a narrow beam in order to overcome high attenuation at mmWaves. The direction of maximum beam gain in beam squint varies with frequency. Based on this observation, a new reduced complexity joint OFDM resource allocation and beamforming strategy is proposed, which employs beam squint to maximize system performance using sub-array hybrid precoder at the transmit-

ter to serve a clustered user population greater than the number of RF chains. Numerical results demonstrate that the proposed sequence for designing RF precoder, baseband precoder, and subcarrier allocation using beam squint provides a greater increase in spectral efficiency at mmWaves than at sub-6 GHz.

The fourth part of the dissertation explores the feasibility of using an unmanned aerial vehicle (UAV) as a fronthaul unit at mmWaves and contrasts its performance with that at the sub-6 GHz range for ad hoc communication. The ideal user grouping method in a 3-dimensional environment with UAV-assisted mmWave communications is investigated for a system with a user population much higher than the number of RF chains available at the UAV. Similar to the analysis of multiple RF chains in terrestrial communication, multiple users per beam are served employing OFDMA. The optimal number of RF chains at the UAV is estimated to maximize the sum rate while satisfying minimum user rate specifications with a given UAV power constraint. Since UAV performance is constrained by battery size, so it is assumed that the UAV is equipped with a solar panel to harvest solar energy in order to increase operational hours. The effect of additional weight because of the solar panel on the performance of the UAV is also analyzed.

Finally, the dissertation's last part studies the feasibility of using an existing backscatter device infrastructure in an indoor environment to provide data support to an obstructed user at mmWaves. When in idle mode, the backscatter device is used to reflect the incoming signal to desired direction without modulating the data stream. This is analogous to a distributed reconfigurable intelligent surface (RIS) system in which the tags act as distributed RIS in indoor environment. Both users and backscatter devices in the mmWave range will have multiple antenna elements, increasing the system's complexity. The challenge, however, is to estimate the angle's direction using a single RF chain at the user. Therefore, a link establishment procedure is proposed that includes estimation of angle of arrival using the retro-reflective property of the antenna array, beamforming design at the user, and beamforming at the backscatter devices.

# सार

पांचवीं पीढ़ी (5G+) से परे संचार का उद्देश्य 3-आयामी सर्वव्यापी प्रदान करना है उपकरण प्रसार के कारण उच्च डेटा दरों का समर्थन करने के लिए नेटवर्क। 5G+ की सहायता के लिए संचार, तीन स्पेक्ट्रम बैंड की जांच की जा रही है: उप-6 गीगाहर्ट्ज, मिलीमीटरवेव (mmWave), और टेराहर्ट्ज़ फ्रीक्वेंसी। उच्च आवृत्ति रेंज का लाभ है बढ़ी हुई बैंडविड्थ उपलब्धता, लेकिन इसकी अपनी चुनौतियों का एक सेट भी है जैसे कि वृद्धि सिग्नल क्षीणन, कम सेल रेंज, कम्प्यूटेशनल और हार्डवेयर जटिलताओं में वृद्धि, और हार्डवेयर लागत में वृद्धि हुई। हालाँकि, पर्याप्त शोध किया गया है उच्च आवृत्तियों पर संचार की व्यवहार्यता प्रदर्शित करने के लिए। यह शोध प्रबंध विशेष रूप से अलग-अलग के तहत उपयोगकर्ताओं की सेवा के लिए एमएमवेव-सक्षम संचार पर ध्यान केंद्रित करता है 2-आयामी और साथ ही 3-आयामी नेटवर्क। रेडियो आवृत्ति की संख्या (आरएफ) श्रृंखलाएं जिन्हें डिवाइस पर तैनात किया जा सकता है, एमएमवेव रेंज में एक बाधा है उच्च हार्डवेयर बिजली की खपत और हार्डवेयर जटिलता के लिए। यह, बदले में, प्रस्तुत करता है प्रीकोडर और कंबाइनर डिजाइन करने में चुनौतियां, पैरामीटर अनुमान, सिग्नल प्रोसेसिंग, और उपयोगकर्ता शेड्यूलिंग। इसलिए, इस शोध प्रबंध का उद्देश्य जांच करना है और डिजाइन ऊर्जा और वर्णक्रमीय रूप से कुशल कम जटिलता स्थलीय और हवाई mmWave संचार ढांचे/आर्किटेक्चर सीमित संख्या में आरएफ श्रृंखलाओं के साथ।

पहला विषय द्वि-आयामी बहु-उपयोगकर्ता के लिए सेक्टर-सेल ढांचे की जांच करता है स्थलीय mmWave संचार जब उपयोगकर्ता जनसंख्या की संख्या से अधिक हो जीएनओडीबी पर उपलब्ध आरएफ चैन। इस ढांचे का विश्लेषण एक के संदर्भ में किया जाता है आरएफ श्रृंखला जो एक सेल के सभी क्षेत्रों को समान क्षेत्र के साथ राउंड-रॉबिन तरीके से सेवा प्रदान करती है ठहरने का समय। विचार यह है कि सेल को समान क्षेत्रों में विभाजित किया जाए और कई की सेवा की जाए एक साथ उपयोगकर्ता जो एक ही स्टीयरेबल का उपयोग करके किसी दिए गए युग में प्रत्येक क्षेत्र में आते हैं पर एक आरएफ श्रृंखला के लिए युग्मित एक समान रैखिक एंटीना सरणी से उत्पन्न बीम gNodeB. नतीजतन, बड़ी संख्या में उपयोगकर्ताओं को सीमित संख्या में आरएफ के साथ सेवा दी जाती है जंजीर। ऑर्थोगोनल के संयुक्त संसाधन आवंटन के लिए एक अनुकूलन समस्या तैयार की जाती है एक सेक्टर और सेक्टर में उपयोगकर्ताओं के लिए फ्रीक्वेंसी डिवीजन मल्टीपल (ओएफडीएम) प्रतीक औसत दीर्घकालिक उपयोगकर्ता दर और सिस्टम ऊर्जा को अधिकतम करने के लिए बीमविड्थ अनुकूलन क्षमता। सिमुलेशन परिणामों के माध्यम से, यह सत्यापित किया जाता है कि कई उपयोगकर्ताओं को

सेवा प्रदान की जा रही है ऑर्थोगोनल फ्रीक्वेंसी डिवीजन मल्टीपल एक्सेस एक सिंगल आरएफ चैन के साथ एक सेक्टर सेल सिस्टम मॉडल एक समय में प्रति आरएफ श्रृंखला एकल उपयोगकर्ता की सेवा से बेहतर प्रदर्शन प्राप्त करता है। इसके अतिरिक्त, इष्टतम बीमविद्युत पर स्थानीयकरण त्रुटि का प्रभाव, जिसके परिणामस्वरूप स्थिति अनुमान से भी अध्ययन किया जाता है।

शोध प्रबंध का दूसरा भाग सेक्टर-सेल ढांचे के अध्ययन का विस्तार करता है gNodeB पर एकाधिक RF श्रृंखलाओं के मामले में एकल RF श्रृंखला के साथ। इसके कम होने के कारण जटिलता, उप-सरणी आधारित या आंशिक रूप से जुड़े हाइब्रिड प्रीकोडर को माना जाता है जो प्रत्येक आरएफ श्रृंखला, एक अलग एंटीना सरणी से जुड़ा हुआ है, एक स्टीयरेबल बीम उत्पन्न करता है। विशेष रूप से, साइडलोब्स की उपस्थिति समवर्ती बीम के दौरान इंटर-बीम हस्तक्षेप का कारण बनती है कई आरएफ श्रृंखलाओं से उत्पन्न होते हैं। इसलिए, इष्टतम बीमविद्युत का अनुमान है इंटर-बीम हस्तक्षेप और बीम स्किंट के लिए लेखांकन करते समय। इसके अलावा, एक इष्टतम जीएनओडीबी में आरएफ श्रृंखलाओं की संख्या का अनुमान आरएफ में बिजली की बर्बादी के हिसाब से लगाया जाता है इकाइयों। सेक्टर-सेल ढांचे के लिए एक परिवर्तनीय समय सीमा संरचना भी प्रस्तावित है परिवर्तनीय संचरण समय अंतराल के साथ एक स्टैंडअलोन एमएमवेव संचार प्रणाली इकाइयां एक ओएफडीएम प्रतीक जितनी छोटी होती हैं। उन्नत मोबाइल के लिए फ्रेम संरचना ब्रॉडबैंड (eMBB) सेवाएं आमतौर पर निश्चित संख्या में OFDM वाले स्लॉट से बनी होती हैं प्रतीक, और सबसे छोटी संचरण समय अंतराल इकाई एक स्लॉट अवधि के बराबर है, रिलीज में तीसरी जनरेशन पार्टनरशिप प्रोजेक्ट (3GPP) न्यू रेडियो (NR) द्वारा परिभाषित के रूप में 15. इसके अलावा, 3GPP दिशानिर्देशों ने इसके लिए एक अलग बीम प्रबंधन चरण का सुझाव दिया है उपयोग किए जाने वाले सर्वोत्तम gNodeB-उपयोगकर्ता बीम जोड़ी को स्थापित करने के लिए प्रारंभिक gNodeB-उपयोगकर्ता बीम जोड़ी डेटा ट्रांसमिशन मोड में बाद के डेटा ट्रांसफर के लिए। बीम प्रबंधन के दौरान चरण, उपयोगकर्ताओं को चैनल देने से पहले संकीर्ण बीम को क्षेत्र को कई बार स्कैन करना चाहिए पहुँच। नतीजतन, अलग बीम प्रबंधन के साथ एक निश्चित फ्रेम संरचना का उपयोग करना और डेटा ट्रांसमिशन चरण महत्वपूर्ण प्रारंभिक पहुँच विलंब का कारण बनता है। इसके अलावा, क्योंकि बीम सर्च ऑपरेशंस, वाइडबैंड एमएमवेव के लिए बीम ट्रेनिंग ओवरहेड अक्सर कम होता है बीम प्रशिक्षण चरण के दौरान चैनल का कम उपयोग किया जाता है। इसलिए, एक संशोधित क्षेत्रवार प्रारंभिक पहुँच प्रक्रिया प्रस्तावित है, जो प्रारंभिक पहुँच विलंब को कम करती है और बैंडविद्युत उपयोग में वृद्धि। प्रस्तावित परिवर्तनीय समय सीमा संरचना, साथ में संशोधित प्रारंभिक पहुँच प्रक्रिया, एक बेहतर औसत और ज्यामितीय माध्य प्रदान करती है लंबी अवधि की उपयोगकर्ता दरों में, विशेष

रूप से गैर-सजातीय उपयोगकर्ता वितरण के मामले में क्षेत्र।

शोध प्रबंध के तीसरे भाग में वाइडबैंड में बीम स्किंट के प्रभाव का विस्तार से अध्ययन किया गया है एमएमवेव संचार। बीम स्किंट प्रभाव बड़ी संख्या के उपयोग के कारण होता है एक संकीर्ण बीम उत्पन्न करने के लिए प्रति आरएफ श्रृंखला से जुड़े एंटीना तत्वों की संख्या mmWaves पर उच्च क्षीणन पर काबू पाएं। बीम में अधिकतम बीम लाभ की दिशा भंगापन आवृत्ति के साथ बदलता रहता है। इस अवलोकन के आधार पर, एक नया कम जटिल जोड़ओएफडीएम संसाधन आवंटन और बीमफॉर्मिंग रणनीति प्रस्तावित है, जो बीम को नियोजित करती है ट्रांसमीटर पर उप-सरणी हाइब्रिड प्रीकोडर का उपयोग करके सिस्टम प्रदर्शन को अधिकतम करने के लिए भंगापन आरएफ श्रृंखलाओं की संख्या से अधिक संकुल उपयोगकर्ता आबादी की सेवा करने के लिए। न्यूमेरिकल परिणाम प्रदर्शित करते हैं कि आरएफ प्रीकोडर, बेसबैंड प्रीकोडर डिजाइन करने के लिए प्रस्तावित अनुक्रम, और बीम स्किंट का उपयोग करते हुए सबकैरियर आवंटन वर्णक्रमीय में अधिक वृद्धि प्रदान करता है उप -6 गीगाहर्ट्ज की तुलना में एमएमवेव्स पर दक्षता।

शोध प्रबंध का चौथा भाग मानव रहित हवाई का उपयोग करने की व्यवहार्यता की पड़ताल करता है mmWaves पर एक फ्रंटहॉल इकाई के रूप में वाहन (यूएवी) और उसके साथ इसके प्रदर्शन की तुलना करता है तदर्थ संचार के लिए उप-6 गीगाहर्ट्ज रेंज में। ए में आदर्श उपयोगकर्ता समूहीकरण विधि यूएवी-समर्थित एमएमवेव संचार के साथ 3-आयामी वातावरण की जांच की जाती है उपलब्ध आरएफ श्रृंखलाओं की संख्या की तुलना में बहुत अधिक उपयोगकर्ता आबादी वाली प्रणाली के लिए यूएवी। स्थलीय संचार में एकाधिक आरएफ श्रृंखलाओं के विश्लेषण के समान, एकाधिक प्रति बीम उपयोगकर्ताओं को OFDMA नियोजित किया जाता है। आरएफ श्रृंखलाओं की इष्टतम संख्या न्यूनतम उपयोगकर्ता दर विनिर्देशों को संतुष्ट करते हुए यूएवी को योग दर को अधिकतम करने का अनुमान है किसी दिए गए यूएवी पावर की कमी के साथ। चूंकि यूएवी का प्रदर्शन विवश है बैटरी का आकार, इसलिए यह माना जाता है कि यूएवी सौर फसल के लिए सौर पैनल से लैस है परिचालन घंटे बढ़ाने के लिए ऊर्जा। अतिरिक्त वजन के प्रभाव के कारण यूएवी के प्रदर्शन पर सौर पैनल का भी विश्लेषण किया जाता है।

अंत में, निबंध का अंतिम भाग मौजूदा बैकस्केटर का उपयोग करने की व्यवहार्यता का अध्ययन करता है किसी बाधित को डेटा समर्थन प्रदान करने के लिए एक इनडोर वातावरण में उपकरण अवसंरचना एमएमवेव्स पर उपयोगकर्ता। निष्क्रिय मोड में होने पर, बैकस्केटर डिवाइस का उपयोग इनकमिंग को दर्शाने के लिए किया जाता है डेटा स्ट्रीम को संशोधित किए बिना वांछित दिशा में संकेत।

यह ए के अनुरूप है वितरित पुनर्विन्यास योग्य बुद्धिमान सतह (आरआईएस) प्रणाली जिसमें टैग वितरित के रूप में कार्य करता है इनडोर वातावरण में आरआईएस। mmWave में उपयोगकर्ता और बैकस्केटर डिवाइस दोनों रेंज में कई एंटेना तत्व होंगे, जो सिस्टम की जटिलता को बढ़ाएंगे। चुनौती, हालाँकि, उपयोगकर्ता पर एकल RF श्रृंखला का उपयोग करके कोण की दिशा का अनुमान लगाना है। इसलिए, एक लिंक स्थापना प्रक्रिया प्रस्तावित है जिसमें कोण का अनुमान शामिल है एंटेना ऐरे के रेट्रो-रिफ्लेक्टिव गुण का उपयोग करते हुए, बीमफॉर्मिंग डिज़ाइन पर उपयोगकर्ता, और बैकस्केटर उपकरणों पर बीमफॉर्मिंग।

# Contents

<b>List of Figures</b>	<b>vii</b>
<b>List of Tables</b>	<b>xi</b>
<b>1 Introduction</b>	<b>1</b>
1.1 Background . . . . .	1
1.2 Beamforming at mmWaves . . . . .	2
1.3 Prior Art on Beamforming at mmWaves . . . . .	4
1.3.1 Beamforming in Wideband mmWave System . . . . .	4
1.3.2 Beamforming for UAV-assisted Wideband mmWave System . . . . .	5
1.3.3 Beamforming for RIS-assisted Wideband mmWave System . . . . .	6
1.4 Other Beamforming Elements Addressed in This Dissertation . . . . .	7
1.4.1 Effect of Wideband mmWave Channel on Beamforming: Beam Squint . . . . .	7
1.4.2 Medium Access Control (MAC) Layer Aspects of Beamforming . . . . .	8
1.5 Research Gaps and Problem Identification . . . . .	9
1.6 Organization . . . . .	11
<b>2 Optimal Beamforming with Single Beam for Multi-user Wideband mmWave Communications</b>	<b>13</b>
2.1 Introduction . . . . .	13
2.1.1 Contribution . . . . .	15
2.1.2 Chapter Organization . . . . .	16
2.2 System Model . . . . .	16
2.2.1 mmWave Channel Model . . . . .	17
2.3 Problem Formulation and Analysis . . . . .	18

2.3.1	Optimal Sectorization Scheme with Perfect UE Location Information . . . . .	19
2.3.1.1	Instantaneous Sum Rate Maximization per Sector . . . . .	19
2.3.1.2	Sector Beamwidth Optimization . . . . .	23
2.3.1.3	Variable Time Scheduling . . . . .	26
2.3.2	Optimal Sectorization Scheme with Estimated UE Position Information . . . . .	29
2.3.3	Complexity analysis . . . . .	32
2.3.3.1	Subcarrier and Power Allocation . . . . .	32
2.3.3.2	Sectorization . . . . .	33
2.3.3.3	Reduced-complexity Method . . . . .	33
2.4	Simulation Results and Discussion . . . . .	33
2.4.1	Optimal sectorization scheme with perfect UE location information . . . . .	34
2.4.1.1	Sub-optimum Resource Allocation per Sector . . . . .	34
2.4.1.2	Fixed Time Scheduling . . . . .	34
2.4.1.3	Variable Time Scheduling . . . . .	36
2.4.2	Optimal Sectorization Scheme with Estimated UE Position Information . . . . .	37
2.5	Summary . . . . .	39
A.	Proof of Lemma 1 . . . . .	40
B.	Derivation of Array Gain . . . . .	41
C.	Proof of Lemma 2 . . . . .	42
<b>3</b>	<b>Multi-RF Beamforming for Multi-user Wideband mmWave Communications</b> . . . . .	<b>45</b>
3.1	Introduction . . . . .	45
3.1.1	Contribution . . . . .	47
3.1.2	Chapter Organization . . . . .	48
3.2	System Model . . . . .	48
3.2.1	UE Deployment . . . . .	49
3.2.2	Spatial Multiplexing with $N_{\text{RF}}$ Beams . . . . .	49
3.2.3	Wideband mmWave Channel Model . . . . .	50
3.2.4	Effective Rate in Presence of Side-lobe Interference . . . . .	51
3.2.5	RF Chain Power Consumption . . . . .	52
3.3	Proposed Variable Time Frame Structure . . . . .	53

3.3.1	3GPP NR IA Procedure . . . . .	53
3.3.2	Proposed IA procedure . . . . .	54
3.3.3	Performance Metrics . . . . .	56
3.3.3.1	IA Delay . . . . .	56
3.3.3.2	Bandwidth Savings . . . . .	57
3.4	Problem Formulation and Performance Evaluation . . . . .	58
3.4.1	Resource Allocation and Cell Sweeping Schemes . . . . .	59
3.4.1.1	Subcarrier and Power Optimization . . . . .	59
3.4.1.2	Cell sweeping schemes . . . . .	61
3.4.2	Joint Estimation of Number of Sectors and Concurrent Beams . . . . .	63
3.4.3	Optimal Sector Sojourn Time Estimation for Non-homogeneous UE Distribution . . . . .	64
3.5	Complexity Analysis . . . . .	66
3.5.1	Subcarrier and Power Allocation per Sector . . . . .	67
3.5.2	Cell Wweeping Schemes . . . . .	67
3.5.3	Estimation of Sector Sojourn Time . . . . .	67
3.6	Results and Discussions . . . . .	67
3.6.1	Performance Evaluation of the Proposed Frame Structure . . . . .	69
3.6.1.1	IAD . . . . .	69
3.6.1.2	Multiple UEs per Beam . . . . .	69
3.6.2	Optimum $S^*$ and $N_{RF}^*$ for Homogeneous UE Distribution . . . . .	70
3.6.3	Optimal Sector Sojourn Time Estimation for Non-homogeneous UE Distribution using WRR . . . . .	73
3.7	Summary . . . . .	73
A.	Proof of $\int_{\hat{\phi}} \mathcal{Q}(ar(\hat{\phi}))d\hat{\phi} = 1$ . . . . .	74
B.	Proof of Lemma 1 . . . . .	75
C.	Calculation of Processing Time . . . . .	76
<b>4</b>	<b>Joint Beamforming and Subcarrier Allocation with Beam Squint in Wide- band mmWave Communication Systems</b> . . . . .	<b>79</b>
4.1	Introduction . . . . .	79
4.1.1	Chapter Organization . . . . .	81
4.2	System Model . . . . .	81
4.2.1	Channel Model . . . . .	81

4.2.2	Precoder . . . . .	82
4.2.3	Achievable Rate . . . . .	83
4.3	RF-SC-BB Design . . . . .	84
4.3.1	Problem Formulation . . . . .	84
4.3.2	RF Precoder Design and SC Allocation . . . . .	84
4.3.3	BB Precoder Design . . . . .	86
4.4	Complexity Analysis . . . . .	87
4.5	Simulation and Results . . . . .	88
4.6	Summary . . . . .	91
<b>5</b>	<b>Sustainable UAV-assisted Multi-user Wideband mmWave Communications</b>	<b>93</b>
5.1	Introduction . . . . .	93
5.1.1	Contributions . . . . .	95
5.1.2	Chapter Organization . . . . .	96
5.2	System Model . . . . .	96
5.2.1	mmWave UAV Communication System Model . . . . .	96
5.2.2	Power Consumption Model . . . . .	98
5.2.2.1	Power Consumed in Transmission . . . . .	98
5.2.2.2	Power Consumption in RF Module . . . . .	98
5.2.2.3	Power Consumption in UAV Motion . . . . .	98
5.3	UE Grouping and RF Precoder Design . . . . .	100
5.4	Subcarrier and Baseband Precoder Design with QoS Constraint . . . . .	102
5.4.1	Problem Formulation . . . . .	102
5.4.2	Proposed Subcarrier Allocation and Baseband Precoder Design . . . . .	104
5.4.2.1	Part 1: Initial Subcarrier Allocation . . . . .	105
5.4.2.2	Joint Baseband Precoding and Subcarrier Reallocation . . . . .	106
5.4.3	Complexity Analysis . . . . .	109
5.5	UAV Solar Panel Design . . . . .	110
5.5.1	Battery Weight . . . . .	111
5.5.2	Solar Panel Weight . . . . .	112
5.6	Results and Discussion . . . . .	113
5.6.1	Sectorization versus $k$ -means Clustering at mmWaves . . . . .	113
5.6.2	Performance of Proposed Joint Subcarrier and Baseband Precoder Algorithm . . . . .	116

---

5.6.3	Optimal $N_B$ Selection at mmWaves . . . . .	117
5.6.4	Analysis of Solar Panel Design at mmWaves . . . . .	118
5.6.5	UAV Communication Performance Comparison at Sub-6 GHz Versus at mmWaves . . . . .	119
5.7	Summary . . . . .	120
<b>6</b>	<b>Reduced Complexity Beamforming for RIS-assisted Indoor mmWave Com- munications</b> . . . . .	<b>121</b>
6.1	Introduction . . . . .	121
6.1.1	Contributions . . . . .	123
6.1.2	Chapter Organization . . . . .	123
6.2	System Model . . . . .	123
6.3	Link Establishment Procedure . . . . .	126
6.4	AoA Estimation . . . . .	127
6.4.1	CRLB Analysis . . . . .	129
6.5	Steering Vector Optimization . . . . .	130
6.6	Results and Discussions . . . . .	131
6.7	Summary . . . . .	134
<b>7</b>	<b>Concluding Remarks and Future Works</b> . . . . .	<b>135</b>
7.1	Concluding Remarks . . . . .	135
7.2	Future Works . . . . .	137
	<b>Bibliography</b> . . . . .	<b>139</b>
	<b>Publications</b> . . . . .	<b>153</b>
	<b>Biodata of the Author</b> . . . . .	<b>155</b>

# List of Figures

2.1	Pictorial representation of a 2-D single cell with 20 independent and uniformly distributed UEs, served by a single analog beam in two consecutive epochs when the cell sectorization scheme is $S = 12$ sectors. Here, sector $S_8$ and $S_{11}$ do not have any UEs. . . . .	17
2.2	(a) Pictorial representation of true position $\mathbf{X}$ and estimated position $\mathbf{X}'$ of a UE along with the actual beam coverage region considering practical radiation pattern. (b) Demonstration of EAoA of the UE; $\Psi$ is the true EAoA and $\Psi_e$ is the estimated EAoA with respect to sector 2, whereas $\Psi_a$ is the true EAoA of UE with respect to sector 1. . . . .	29
2.3	Sector sum rate versus number of UEs plot for optimal and sub-optimal resource allocation techniques. . . . .	34
2.4	(a) Average long-run UE rate versus total number of sectors plot for uniformly distributed UE population; (b) gNB energy efficiency versus total number of sectors plot for uniformly distributed UE population. (c) Pareto front for average long-run UE rate and gNB energy efficiency optimization.	35
2.5	(a) Plot of sum rate per sector versus number of UEs in the sector for three different sectorization schemes. (b) Comparison of optimal $S^*$ obtained through exhaustive search method and sub-optimal $\hat{S}^*$ obtained using reduced complexity search method for uniform and non-uniform UE distribution. . . . .	36

2.6	Improvement in of $\bar{R}$ and $\bar{E}$ using variable time scheduling scheme over fixed time scheduling scheme. (a) shows the improvement in maximum achievable average long-run UE rate for different UE population, using variable time scheduling scheme with $[\alpha = \alpha_R, S = S'^*]$ over fixed time scheduling scheme at $[\alpha = \alpha_0, S = S^*]$ ; and (b) shows the improvement in maximum achievable gNB energy efficiency using variable time scheduling scheme with $[\alpha = \alpha_E, S = S''^*]$ over fixed time scheduling scheme at $[\alpha = \alpha_0, S = S^*]$ . . . . .	37
2.7	(a) Position error bound of $\bar{\Psi}_e$ versus number of sectors in worst-case scenario. $PEB_a$ is the PEB obtained using (2.40); $PEB_b$ is the PEB achieved in [62]. (b) Percentage of UEs lying in the beam overlapping region due to localization error. . . . .	38
2.8	Average long-run UE rate versus total number of sectors plot for (a) 1000 UEs uniformly distributed in the cell, and (b) 500 UEs non-uniformly distributed in the cell with probability of distribution of UEs in a 6 non-overlapping zones of the being $[0.9, 0.05, 0.03, 0.01, 0.008, 0.002]$ . . . . .	38
3.1	(a) and (b) depicts round-robin scheduling of sectors over two consecutive epochs with $S = 12$ sectors and $N_{RF} = 4$ beams, represented as $\{S1, \dots, S12\}$ and $\{B1, \dots, B4\}$ , respectively. Here, $S_{b=B1} = \{S1, S2, S3\}$ ; and (c) shows steering directions $\{R1, \dots, R8\}$ of a UE within beam B1, i.e., $S_r = 8$ . . . . .	50
3.2	(a) Steps in IA for new UEs using 3GPP NR guidelines (b) Steps in IA for news UEs according to proposed frame structure for directional cellular communication. . . . .	54
3.3	Schematic diagram of the proposed frame structure, transmitted in $s$ th sector, depicting the position of control channels required for IA in $\tau$ duration, and control channels required for contention resolution and UE beam refinement in $T$ duration. . . . .	55
3.4	$P_{peak}$ versus sectorization scheme for different $N_{RF}$ . . . . .	64
3.5	(a) Improvement in IAD with $N_{rep} = 17$ using proposed IA procedure over the 3GPP NR. $N_{rep} = 17$ is equivalent to using full 1 GHz bandwidth for SS blocks. (b) Saving in bandwidth using proposed IA procedure over the 3GPP NR. . . . .	69

3.6	Comparison of (a) average long-run UE rate and (b) gNB energy efficiency with the existing protocols and proposed protocol. Here, $ \mathcal{S}_b  = 5$ and $S_r = 12$ . . . . .	69
3.7	(a) EIRP level in main-lobe and side-lobes in a beam at different beamwidth. (b) Normalized interference experienced by a UE with respect to variable HPBW. (c) Convergence of peak sector sum rate in an epoch using Algorithm 3.2 for $S = 30$ and $M = 100$ . . . . .	70
3.8	Illustration of $\bar{R}$ as a function of $S$ and $N_{RF}$ . . . . .	71
3.9	Comparison of achievable $\bar{R}$ of the proposed system model with the schemes in [19,84,85] and multi-RF MMSE method for $M = 100$ . . . . .	72
3.10	Comparison of (a) $\bar{R}$ and (b) normalized $\bar{G}$ for $M = 100$ non-homogeneously distributed UE achieved with 3GPP NR, synchronous and asynchronous schemes. . . . .	73
B3.1	(a) $\Pr_c$ and (b) $\mathbb{E}[\Pr_c]$ of new UEs arriving during $T_{tot} = 100$ ms. . . . .	76
4.1	Illustration of beam squinting effect at 28 GHz with $N_{RF} = 1$ connected to $N_t$ antennas and steered at $80^\circ$ . . . . .	82
4.2	(a) Spectral efficiency comparison of RF-SC-BB and benchmark SC-RF-BB approaches at 28 GHz. (b) Gain in spectral efficiency using RF-SC-BB over RF-SC-BB with approach at 28 GHz and 5 GHz. . . . .	89
4.3	Illustration of beam squinting effects at 5GHz and 28GHz with $N_t^{5GHz} = 2$ , $N_t^{28GHz} = 32$ , and steering angle = $80^\circ$ . . . . .	90
4.4	Comparison of normalized geometric mean rate of RF-SC-BB and SC-RF-BB (B1) approaches at 28 GHz. . . . .	90
5.1	(a) Illustration of UE grouping to partition UEs into $N_B^{k\text{-means}} = 3$ groups using $k$ -means clustering. (b) Geometric illustration of steering angles and beamwidth in azimuth and elevation planes. . . . .	101
5.2	Illustration of UE grouping by partitioning the area into $N_B^{\text{sector}} = 8$ sectors with each sector served by one RF beam. . . . .	115
5.3	Plot of gain in geometric mean rate $\Delta G_R$ achieved by using $k$ -means clustering over sectoring approach at mmWaves, given $P_{limit} = 5$ W and $N_B = N_B^{k\text{-means}} = N_B^{\text{sector}}$ . . . . .	115

5.4	(a) Comparison of UE rates achieved with proposed joint subcarrier and baseband design algorithm and penalty based design algorithm at mmWaves. (b) Illustration of the convergence of rate of UEs with penalty based design algorithm. Here, rate convergence of only those UEs is shown that initially had $R_k^j < R_0$ .	116
5.5	(a) Performance comparison of the proposed subcarrier and precoder algorithm over the benchmark scheme [29] at mmWaves, given $P_{limit} = 5$ W. (b) Illustration of geometric mean rate $\bar{R}$ as a function of number of beams $N_B$ at mmWaves, given $P_{limit} = 5$ W, and $\chi = 1$ .	117
5.6	Plot of optimal $N_B^*$ value as a function of available power $P_{limit}$ for transmission module at UAV at mmWave range for $\chi = 1$ .	117
5.7	(a) Convergence of $P_{hover}$ and $\mathcal{N}_{ser}$ when $P_{Tot} = 5$ W. (b) Illustration of energy efficiency of UAV with and without considering solar panels weight optimization.	118
5.8	Comparison of $\bar{R}$ at sub-6 GHz and mmWaves at the UAV as a function of $P_{limit}$ and illustration of $P_B$ at sub-6 GHz. Here, $\chi = 1$ , $R_0 = 1$ Mbps, $N_B^{sub} = 6$ , and $N_B^{mm} = N_B^*$ (the optimal value that gives best performance at mmWaves).	119
6.1	Illustration of backscatter-assisted mmWave communications system model with tags configured in retro-reflective mode.	124
6.2	Flowchart for link complete virtual link establishment between AP and UE.	126
6.3	RMSE and AEB of proposed AoA estimator.	132
6.4	Average number of reflecting elements $\bar{N}_T$ aiding AP to UE communication when tags are distributed homogeneously and non-homogeneously with $\lambda = 2$ and $N_T = 8$ .	132
6.5	Reduction in rate when using estimated AoAs as compared to using true AoAs to design tags' reflection coefficients and UE steering direction in case of homogeneously distributed tags.	133
6.6	Comparison of achievable rate with different schemes for homogeneously distributed and non-homogeneously distributed tags.	133

# List of Tables

1.1	Existing MAC protocols for standalone mmWave systems . . . . .	9
3.1	Power consumption of components in a RF chain . . . . .	52
3.2	Simulation parameters and values . . . . .	68
3.3	UE scheduling complexity . . . . .	72
5.1	Some important variable description . . . . .	99
5.2	Power consumption of components in a RF chain. . . . .	100
5.3	UAV design specifications . . . . .	112
5.4	Simulation parameters . . . . .	113
6.1	Simulation parameters . . . . .	131

# List of Symbols

$\mathbf{a} \in \mathbb{R}^{N \times 1}$	A real vector of size $N \times 1$
$\mathbf{A} \in \mathbb{R}^{M \times N}$	A real-valued matrix of size $M \times N$
$\mathbf{0}_{M \times N}$	$M \times N$ matrix of zeros
$\mathbf{I}_N$	$N \times N$ identity matrix
$\mathbf{A}_{m,n}$	$(m, n)^{th}$ element of the matrix $\mathbf{A}$
$\text{Tr}\{\mathbf{A}\}$	Trace of the matrix $\mathbf{A}$
$\mathbf{a}[m]$	$m^{th}$ element of the vector $\mathbf{a}$
$\ \mathbf{a}\ _2$	Standard $l_2$ -norm of the vector $\mathbf{a}$
$(\cdot)^T$	Transpose of the vector/matrix
$(\cdot)^H$	Transpose of the vector/matrix
$(\cdot)^\dagger$	Moore-Penrose pseudo inverse of the vector/matrix
$\text{diag}(\cdot)$	Standard diagonalization operation on a vector
$ \cdot $	Cardinality operation
$\cup$	Set union operation
$\text{dom } f$	Domain of the function $f$
$\mathcal{O}$	Algorithm run-time complexity
$\mathcal{L}(\cdot)$	Lagrangian operator

# List of Abbreviations

mmWave	Millimeter Wave
5G+	Beyond 5th Generation
RF	Radio Frequency
OFDM	Orthogonal Frequency Division Multiplexing
OFDMA	Orthogonal Frequency Division Multiple Access
eMBB	enhanced Mobile Broadband
NR	New Radio
UAV	Unmanned Aerial Vehicle
RIS	Reconfigurable Intelligent Surface
WLAN	Wireless Local Area Network
UE	User Equipment
gNB	gNodeB
LoS	Line-of-Sight
SNR	Signal-to-Noise Ratio
ADC	Analog-to-Digital Converter
DAC	Digital-to-Analog Converter
SDMA	Spatial Division Multiplexing
MIMO	Multiple-Input-Multiple-Output
JSDM	Joint Spatial Division Multiplexing
WMMSE	Weighted Minimum Mean Squared Error
MPC	Multi Path Component
CSI	Channel State Information
SVD	Singular Value Decomposition
ML	Maximum Likelihood
AoA	Angle-of-Arrival
DFT	Discrete Fourier Transform

MUSIC	MUltiple Signal Classification
TTI	Transmission Time Interval
3GPP	3rd Generation Partnership Project
HPBW	Half Power BeamWidth
IA	Initial Access
EIRP	Effective Isotropic Radiated Power
GPS	Global Positioning System
ToA	Time-of-Arrival
QoS	Quality-of-Service
2-D	2-Dimensional
ULA	Uniform Linear Array
NLoS	Non Line-of-Sight
NP	Non-deterministic Polynomial time
KKT	Karush-Kuhn-Tucker
MOP	Multi-objective Optimization Problem
SOP	Single-objective Optimization Problem
FNBW	First Null BeamWidth
EAOA	Effective AoA
CRLB	Cramér-Rao Lower Bound
FIM	Fisher Information Matrix
PEB	Position Error Bound
SA	StandAlone
NSA	Non-StandAlone
UL	UpLink
DL	DownLink
TDMA	Time Division Multiple Access

UMi	Uran-Micro
WRR	Weighted Round Robinn
SS	Synchronization Signal
RACH	Random Access CHannel
PRACH	Physical Random Access CHannel
RAR	Random Access Response
PDCCH	Physical Downlink Control CHannel
PUCCH	Physical Uplink Control CHannel
IAD	Initial Access Delay
IUI	Inter-User Interference
s.t.	such that
UPA	Uniform Planar Array
ZF	Zero-Forcing
MMSE	Minimum Mean Squared Error
PV	PhotoVoltaic
AP	Access Point
OMP	Orthogonal Matching Pursuit
AEB	Angle Error Bound
RMSE	Root Mean Squared Error